LA-UR-22-25796

Approved for public release; distribution is unlimited.

Title: Fourth Generation MPDV and MBR at DARHT

Author(s): Gilbertson, Steve Michael
Payne, Charles Nelson
Kalb, Daniel M.
Schultz, Kimberly Ann

Intended for: Report

Issued: 2022-06-22

Fourth Generation MPDV and MBR at DARHT

Steve Gilbertson, Charles Payne, Dan Kalb. and Kim Schultz

ABSTRACT

A new experimental setup for diagnosing hydrotest performance was designed, built, and implemented at DARHT. The setup consists of 128 points of fourth generation (Gen4) multiplexed photonic Doppler velocimetry (MPDV) and 128 separate points of modulation based ranging (MBR) to serve as a direct complement to the MPDV. The diagnostics were designed to overcome limitations in the third generation of the MPDV diagnostic that limited laser launch power to ~10 mW per point. As the main failure mechanism identified in the third generation MPDV system arose from stimulated Brillouin scattering, a nonlinear optical phenomenon inherent in standard single mode fiber, the fourth generation MPDV system reduced the number of time-multiplexed channels by a factor of two. This has allowed laser launch power to be increased to as much as 200 mW per channel which is a 20 times increase in the signal to noise ratio (SNR) as compared with the third generation system. This document will first discuss the previous limitations and describe the design of the system. This will be followed by the results of a simple flyer plate experiment used to demonstrate the improved SNR as well as calibrate the phase errors in the system that MBR is sensitive to.

INTRODUCTION

Measurements of a dynamic surface that has undergone either an explosion or implosion are critical to the Los Alamos National Lab hydrotest program. The experimental data can be used to directly compare to theoretical predictions and models and serves as a direct validation of hydro codes. Over the past decade these measurements have been made by directly measuring the velocity of a moving surface using the photonic Doppler velocimetry (PDV) technique. The basic idea for the diagnostic is that a continuous wave (CW) laser is sent to a surface which then reflects and is recollected. When the surface of interest is moving, a Doppler shift is imparted to the laser beam that manifests itself as a frequency change from the fundamental frequency of the unshifted laser. The shifted laser is then combined with an unshifted reference laser, thereby generating a GHz-range beat frequency that can be recorded with off-the-shelf detectors and oscilloscopes. A sliding window FFT of the temporally evolving signal gives a continuous high resolution and high sensitivity measurement of the velocity history of the dynamic surface. A simple integration of the velocity will then yield the position of the moving surface which can be directly compared to the theoretical predictions.

As the diagnostic has proven its utility to the hydrotest program over the past decade, the requirements for the number of points has increased. To offset the high cost of the GHz bandwidth scopes, multiplexing techniques have been devised to maximize the number of points that can be recorded on each scope channel. The techniques are referred to as multiplexed photonic Doppler velocimetry (MPDV). For example, the Gen2 MPDV utilized both frequency and time multiplexing. Frequency multiplexing refers to sending multiple laser wavelengths to the same scope channel. These can all be separated via FFT signal analysis. While frequency multiplexing worked well for many years, it is being replaced by solely time-mulitplexed systems. The reason for this is that frequency multiplexed signals share the

dynamic range of the scope at any particular time, thereby reducing the quality of the signals. Additionally, having multiple velocity traces on the same spectrogram can lead to very complicated results. Time multiplexing, on the other hand, refers to sending additional velocity measurements to the same scope channel, but delayed in time with long fiber delays. Both the Gen3 and Gen4 MPDV systems utilize only time multiplexing, with 16 time delayed velocity measurements for the Gen3 systems and 8 measurements for the Gen4 system.

There are, however, two major limitations with the PDV diagnostic. The first is that PDV gives the wrong velocity when the motion of the surface is not parallel to the line of sight of the diagnostic. The PDV optical probe measures only the velocity component that lies along the optical probe pointing vector. If the motion is slightly non radial, the total magnitude of the velocity is lost. Taking this to the extreme, if the motion of a surface is fully orthogonal to the line-of-sight of the PDV probe, the diagnostic will record zero velocity. This will give significant errors in the actual position of the surface. To compensate for this, prior knowledge of the experiment is required which is not always available. Another option however, is to include a separate direct displacement measurement to the surface. The MPDV diagnostic that we field at DARHT therefore includes a modulation based ranging (MBR) diagnostic on every point of PDV. Details of the diagnostic can be found in reference [1]. As a simple explanation, a 15 GHz microwave signal is imparted onto the 1550 nm PDV lasers with a Mach-Zehnder interferometer. This generates two sidebands each 15 GHz separated from the main laser wavelength. All three signals can then generate a separate PDV trace but with a phase relationship between them that can be extracted with simple algebra. The instantaneous phase of this signal can then be extracted and compared to a reference 15 GHz microwave source. Through simple fringe counting of the signal, the displacement to the surface can be directly measured. Since this is measuring the true displacement and not just a component along the line-of-sight, the diagnostic can be used to show the error in the integrated PDV signals with differences attributable to non-radial motion. Figure 1(a) shows a sample spectrogram with MBR and integrated PDV compared. Figure 1(b) shows the results of the velocity extraction (blue line) integrated PDV (red line) and MBR (black dots).

The second limitation is the SNR of the diagnostic. The reflected light from the dynamic surface is usually very dim with typically a 25 dB drop for a static measurement. This can drop considerably more after the surface becomes dynamic. The most obvious way to improve this is by increasing the launch light to the surface. The Gen3 MPDV system has an option of launching either 10 mW per point or 200 mW per point for a theoretical 20-fold increase in SNR. Increasing the launch light remains an option as long as the power remains below the threshold power for nonlinearities in the optical fiber. Unfortunately the onset of nonlinear effects is proportional to the length of the optical medium which can be hundreds of km for a high channel count frequency multiplexed system.

The strongest nonlinear effect that has been observed so far has been stimulated Brillouin scattering (SBS). This effect is a $\chi^{(3)}$ process where $\chi^{(3)}$ is a nonlinear susceptibility tensor that relates the nonlinear polarization of the optical medium to the product of the field amplitudes via constants of proportionality. The explanation for SBS is that when a high intensity laser propagates through a medium, it can back-reflect from imperfections in the fiber. These can be localized impurities or accumulated Rayleigh scattering along the length of the medium. The back reflected light then counter propagates with the incident light thereby setting up a

standing wave interference patter within the fiber. The oscillatory intensity variation within the fiber can then modify the nonlinear refractive index of the medium resulting in a periodic index change. This can be thought of as a Bragg grating that has a grating period optimized to reflect the incident light. This results in a cascading failure of the fiber to propagate additional light.

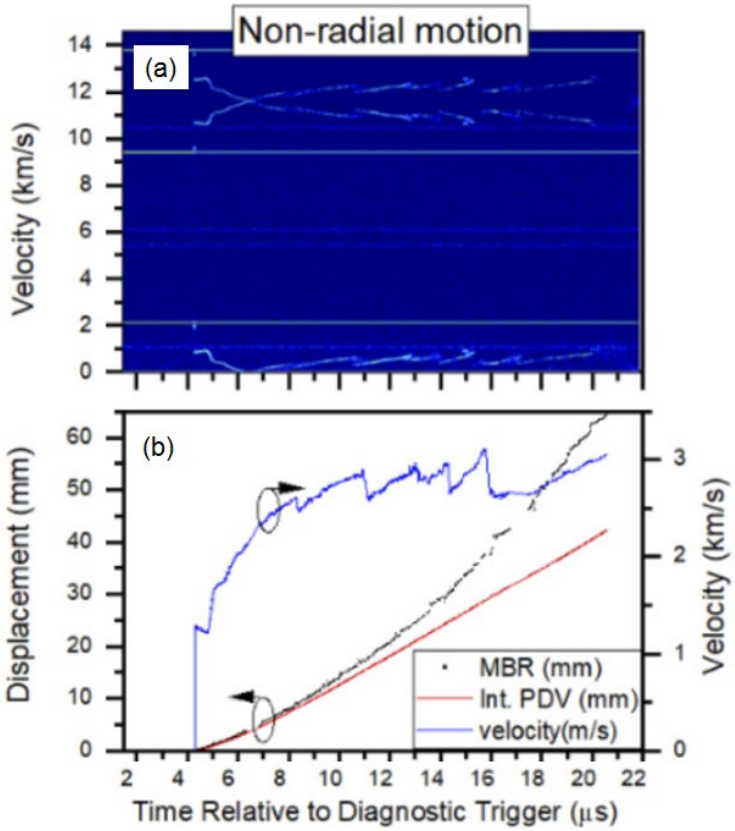

Figure 1 (a) spectrogram showing the velocity of a highly non-radial surface. The velocity at the bottom of the trace is an inverted PDV trace while the two replicas at the top of the trace are associated with the MBR diagnostic. (b) the extracted velocity (blue line) and integrated PDV (red line) along with the extracted displacement from MBR (Black dots). The Integrated PDV underestimates the actual position of the surface nearly 2 cm at the end of the experiment.

Eventually a steady state will occur where any additional light will only be reflected and the output light remains constant and significantly reduced. Since the Gen3 MPDV system was designed as a counter-propagating system, the SBS signal ends up swamping the detectors for other non-SBS related channels representing a significant loss of data. Figure 2 shows a time domain signal that has experienced SBS. As can be seen in the figure, time slices 2 and 3 show a significant amount of noise that was born from a different scope channel undergoing SBS. The noise then counter propagates to these particular time slices. It should be noted that these channels would be lost in the experiment.

The impurities in the fiber also result in photon coupling with the phonon quasiparticle of the fiber. The counter propagating photon can then lose energy to the Stokes SBS components, showing up as a few GHz frequency shifted signal. This gives an additional frequency domain verification that the effect is from SBS. The threshold power for SBS is given by:

$$P_{SBS} \approx \frac{21A_{eff}}{gL_{eff}} \quad (1)$$

where A_{eff} is the effective area of the fiber, L_{eff} is the length, and g is a constant dependent on the optical properties of the medium. Our Gen3 MPDV system has shown SBS at high power when the path length for each consecutive delay has been 20 km. This gives a total length for a 16 channel system as 280 km. However, a 10 km length between temporal windows (total length 140 km) has been shown to exhibit very little SBS. Based on equation 1, we would need to reduce our L_{eff} by a factor of 2. Since the time window lengths are determined by the experiment, this means that we are forced to sacrifice channel counts from the total of 16 channels of Gen3 MPDV to 8 channels in Gen4.

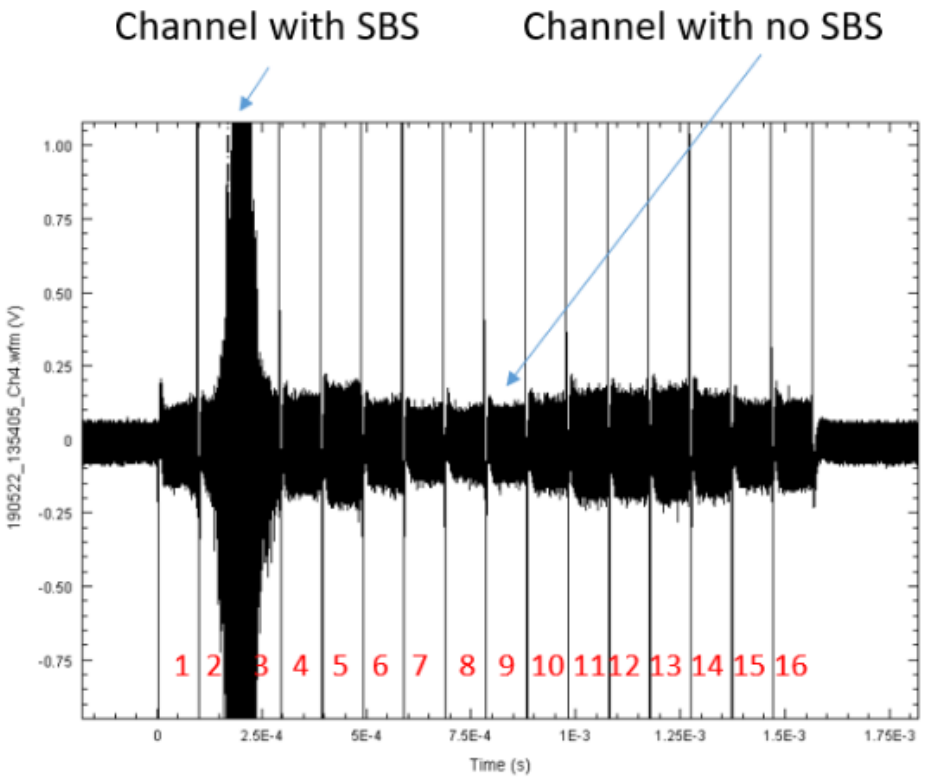

Figure 2 Time domain signal from a Gen3 MPDV system. The signal is divided into 16 separate PDV channels via time multiplexing. Time slices 2-3 show the signature of SBS where the time domain signal is swamped by counter propagating light from another channel.

EXPERIMENTAL SETUP

The Gen3 MPDV diagnostic suffers from SBS due to the design of the reconfigurable optical add/drop delay module (ROADDM). This is because the ROADDM houses the long fiber delays necessary for the time multiplexing. As such, the Gen4 takes advantage of the well-designed probe and control chassis while only requiring a redesigned ROADDM. The new ROADDM design can be seen by the schematic in figure 3. The ROADDM units were built by Dicon Fiberoptics. It is similar to the original Gen3 MPDV ROADDM but reduces the total number of time multiplexed channels to 8 per scope channel. This eliminated the need for ~150km of

optical fiber in the design. An additional benefit is that the erbium doped fiber amplifiers (EDFA) located within the ROADDM no longer need to be two stage as the amount of optical power loss in the system has been reduced by half. The new amplifiers have ~ 3dB less noise as compared to the Gen3 MPDV amplifiers.

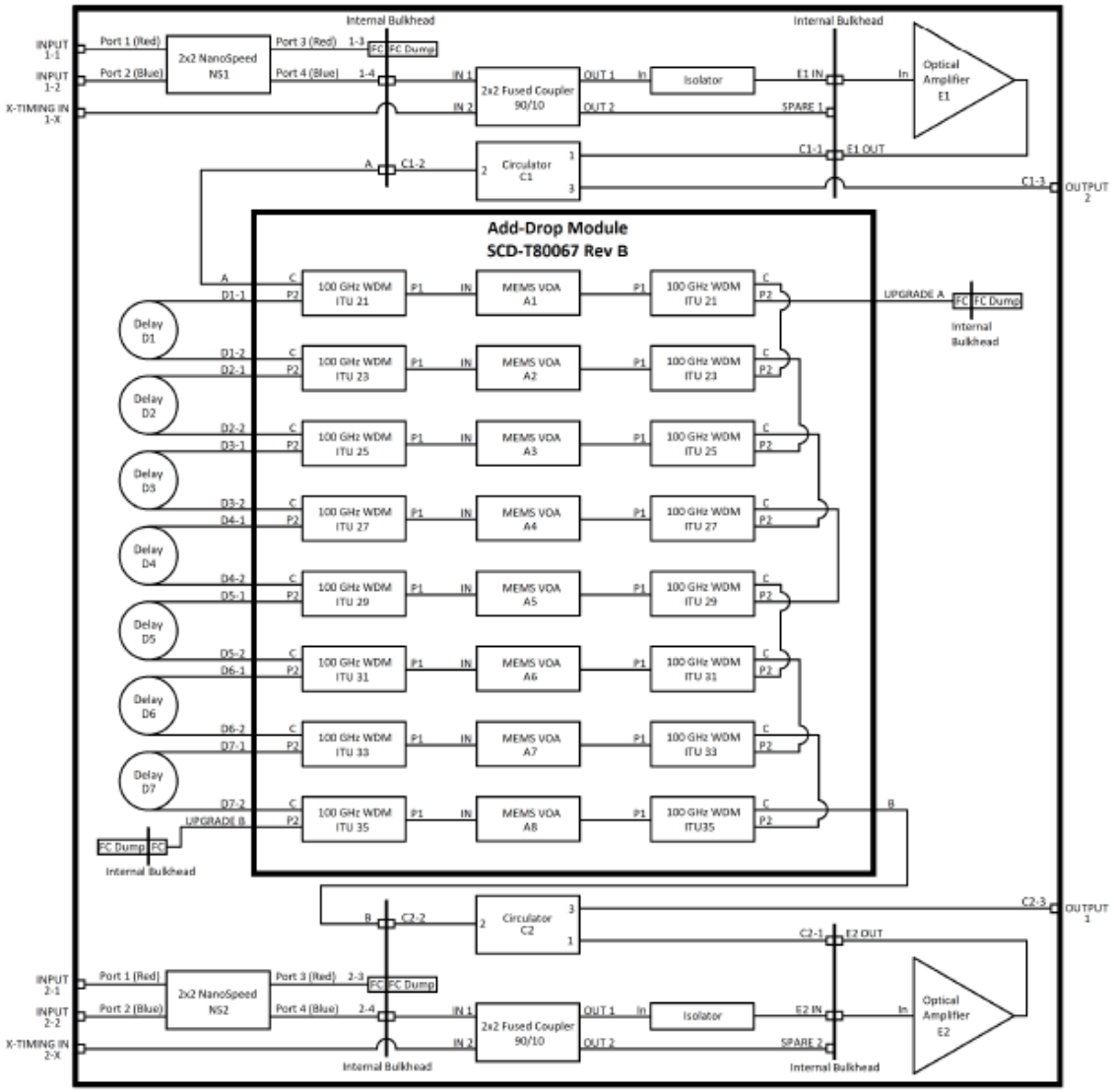

Figure 3 Gen4 MPDV ROADDM schematic as drawn by Dicon.

METHODS

The verification of the functionality of the Gen4 MPDV system consisted of two main steps. First, a channel-by-channel check was conducted to ensure the mapping of all 128 points was understood from the injection of the lasers, all the way through the probe chassis and the newly designed ROADDMs, and finally onto the scope channels. This was conducted by connecting a single probe that sent light to a spinning router operating at ~25,000 RPM. This resulted in a

velocity offset from the baselines by a few 10s of m/s. This offset was observable on every channel and was correctly mapped in every case.

Once the mapping was well understood, a detonator-driven flyer plate experiment was conducted. The flyer plate apparatus is shown in figure 4. The holder was 3-D printed for simplicity. Starting from the bottom of the figure, a detonator (RP-1) initiated a ½" diameter PBX-9501 pellet. A small air gap existed between the pellet and a 0.8 mm thick stainless steel plate. The air gap cushioned the plate so as to reduce the initial acceleration. After initiation, the flyer plate could travel freely over 100 mm towards PDV probes on the opposite side. The probes were positioned as parallel to the direction of motion as possible to eliminate any potential non-radial motion in the experiment.

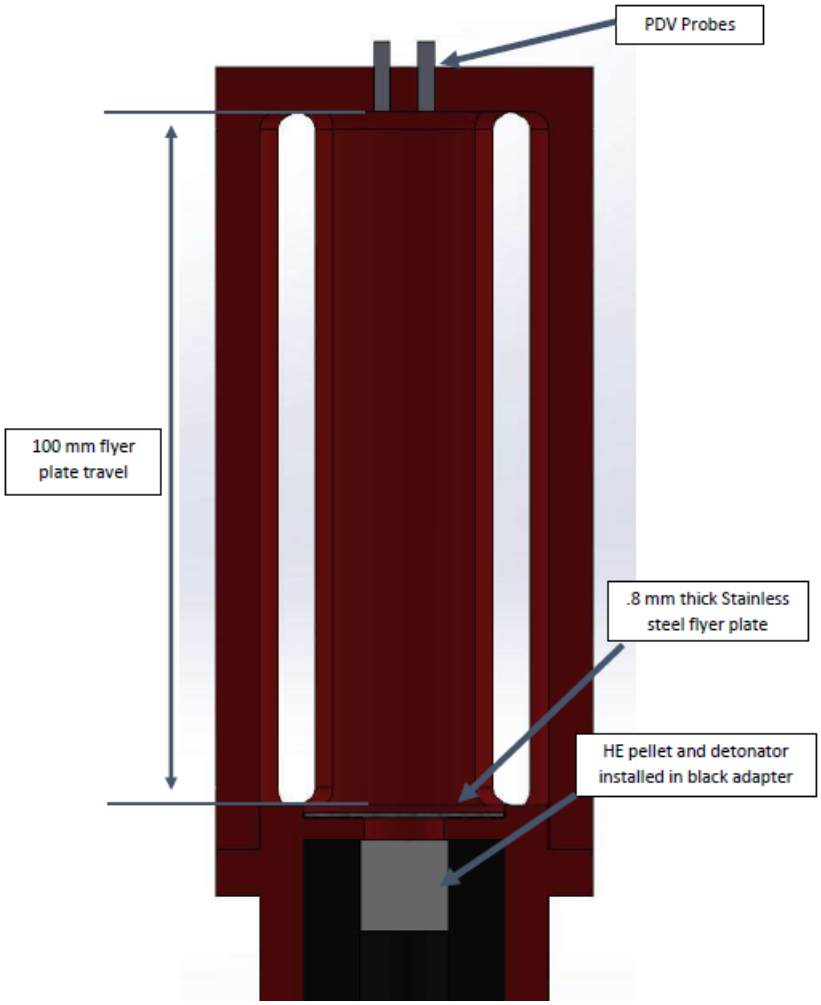

Figure 4 Flyer plate holder and assembly.

The benefit of the flyer plate was two-fold. First, the experiment allowed the system to operate with a velocity more applicable to an actual experiment than what the spinning router could provide. Secondly, the experiment could be used for measuring the amount of material dispersion within the MPDV system, particularly the ROADDMs. This is of critical importance for the MBR diagnostic as it is a phase-sensitive measurement. In order for the flyer plate

experiment to work for the dispersion measurement and calibration, all velocities recorded need to be identical. This would ensure that any phase error observed between any channel and the next would be entirely due to the additional length of fiber between the channels. Figure 5 shows a rough schematic for this setup. Typically, the Gen4 MPDV system would send 8 separate signals out on 8 separate probes via the probe chassis to the surface of interest. The signals would then return to the probe chassis where they would be muxed. The signals would then pass through the ROADDM where they would be time multiplexed, sent back to the probe chassis to be combined with the reference laser, and finally sent to the detector for recording. For the flyer plate experiments, all 8 probe chassis channels for a single scope channel have a full reflector attached. This reflects 100% of the emitted light. The probe chassis still muxes all 8 channels, but before entering the ROADDM, the muxed signal passes through a circulator where it is then sent to a single optical probe on the flyer plate setup. This ensures all 8 velocities on a single scope channel are identical.

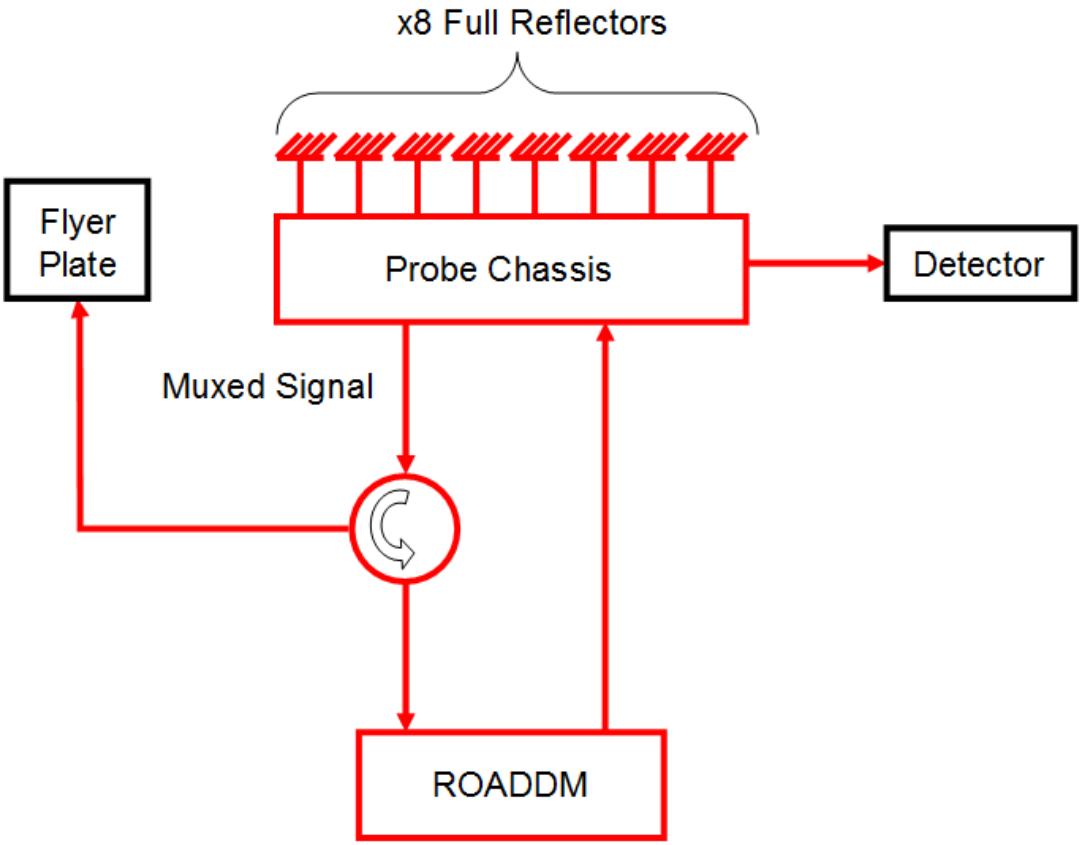

Figure 5 Gen4 MPDV configured for flyer plate testing. The probe chassis has 8 full reflectors. The output muxed signal then passes through a circulator where it is sent to a single probe on the flyer plate setup. The signal then returns to the ROADDM.

RESULTS AND DISCUSSION

The resultant spectrogram for several channels sent to a single optical probe is shown in figure 6. The PDV signals are inverted at the bottom while the MBR signals are located at the top of the traces. All 8 traces are identical as expected. Figure 6(a) shows all 8 channels together.

Figure 6(b) shows a close up of a single time slice. Since each channel's laser power can't be tuned due to a full reflector being added to the output of the probe chassis, the time-slice to time-slice variation in the SNR varies more than in an actual experiment. This only occurs for flyer plate tests however. When analyzing the data, all 8 time slices have easily extractable MBR and PDV data. Figure 6 demonstrates a single ROADDM's data but in reality there was a separate set of flyer plate results for each ROADDM. Since the ROADDMs are counter propagating, each ROADDM separates a total of 16 individual PDV measurements, 8 on 1 scope channel and 8 on another. However, since a ROADDM shares the dispersion modules for the two counter propagating scope channels, only one set of data is required to map the dispersion in each ROADDM.

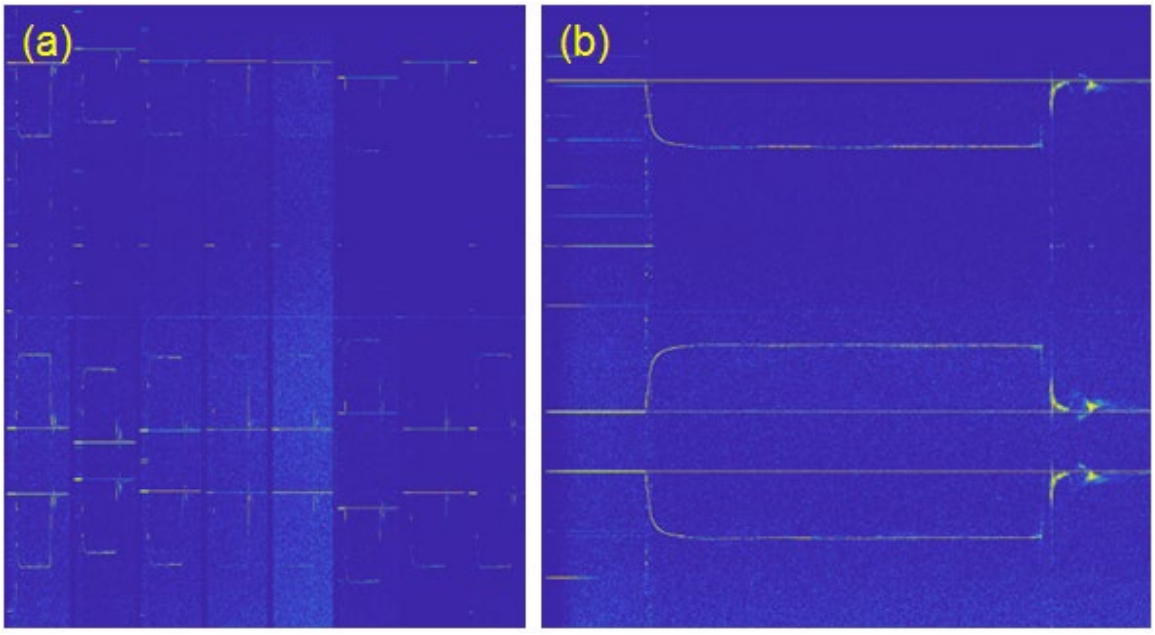

Figure 6. 8 PDV measurements from a single ROADDM. All 8 channels are identical as they all measured velocity along the same PDV probe. The signal strength varies from channel to the next. (b) shows the output of a single time slice. In all cases the PDV and MBR data is fully extractable.

From the experimental data, all 8 MBR traces were next extracted. Details on the analysis of the MBR data can be found in reference 1. A phase correction has to be applied to all MBR data taken on the same scope channel as they all share the same detector. The detectors (Miteq 20 GHz) have a spectrally dependent phase shift. This is measured by splitting the output of our microwave source with half being sent to a modulator with a PDV laser passing through it. The output from the modulator was then sent to one of the photodetectors and recorded on a high bandwidth (23 GHz) scope. The other half of the microwave source was sent to another channel of the scope. The delays and types of cables were kept as similar as possible. The microwave source was then varied from 0 to over 25 GHz in MHz steps. The phase difference was then measured and a correction plot was made. Figure 7 shows a sample phase measurement of a Miteq detector. The phase changes by more than 4 radians over the total bandwidth of the detector. As each of the three traces on a spectrogram (PDV, upper MBR, lower MBR) are located in distinctly different regions of the detector bandwidth, this phase shift was to be taken

into consideration. Additionally, the signals located at the highest frequency change rapidly with a measureable phase shift as the velocity increases. This effect contributes to a significant error in the displacement measurement and needs to be corrected. It should be noted that if all

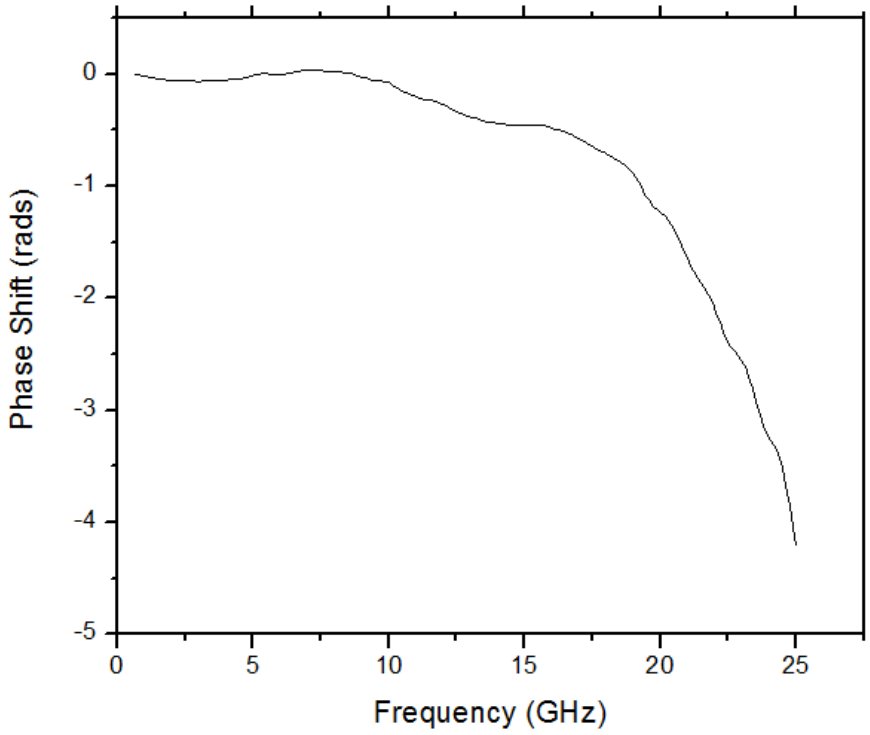

Figure 7. Sample phase correction for a Gen4 MPDV photodetector. The PDV signal and lower MBR are located in relatively flat portions of the plot while the upper MBR phase can change rapidly for frequency changes over a few GHz.

PDV signals were truly identical, a photodetector phase correction would not be required. However, each consecutive temporal slice is detuned slightly from the previous one meaning all signals take up a slightly different portion of the photodetector bandwidth. This is intentional as MBR is exceptionally sensitive to phase errors and bleed though of neighboring signals can negatively effect the phase extraction in any particular time slice. By detuning the reference laser wavelength slightly, each time slice can have a different baseline frequency located a few frequency bins away from any other baseline.

After applying the photodetector phase corrections to the extracted MBR data, the integrated PDV data was subtracted to give the error between the MBR and integrated PDV. As the experiment was specifically designed to be fully radial, the error should be zero. Any remaining error can then be fully attributed to material dispersion in the optical fiber. The phase shift $\phi(\lambda)$ for optical fiber is given by:

$$\phi(\lambda) = \frac{2\pi}{\lambda_0}[n(\lambda_{MBR})L - n(\lambda_0)L] \tag{2}$$

where λ_0 is the PDV laser central wavelength, n is the refractive index as given by a Sellmeier equation, L is the fiber length and λ_{MBR} is the wavelength for the MBR sideband. There are actually 2 sidebands so there is a different wavelength shift for each. While the wavelengths associated with MBR sidebands are only separated by 15 GHz from the main laser wavelength, after many kilometers of fiber length L, these small changes in the wavelength can eventually be significantly dispersed.

Figure 8 (a) shows the resultant error plots of the MBR subtracted from the integrated PDV data for the 8 channels of a single ROADDM. The error is a displacement offset generated by the additional linear dispersion in each consecutive time slice. It can be seen that each consecutive time slice shows a constant offset from the previous time slice which makes sense since each slice sees an integer multiple of 20 km dispersion. The first slice has no dispersion which is why it has no error between the MBR and integrated PDV.

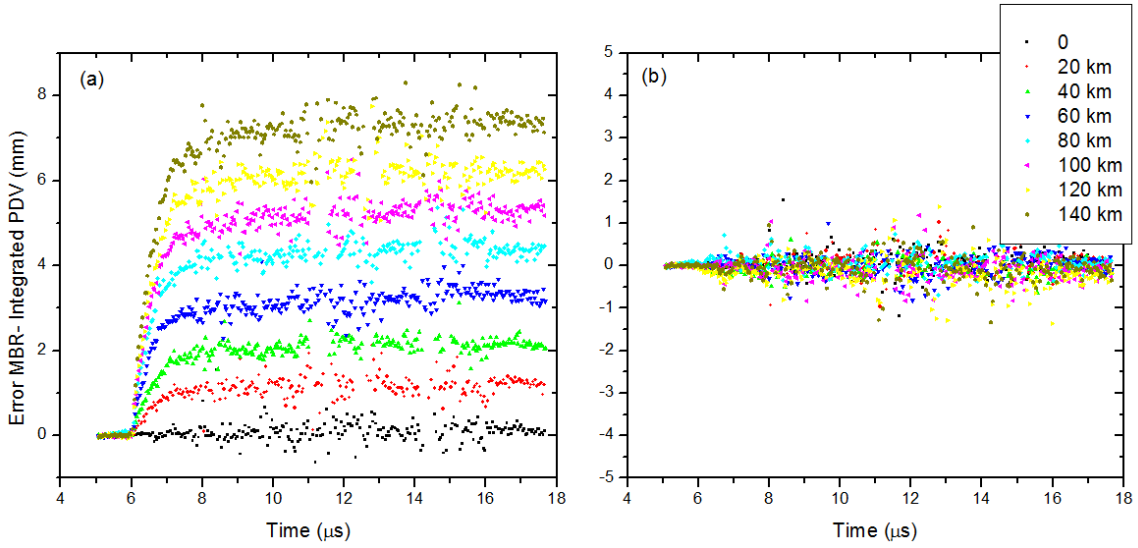

Figure 8 (a) shows the results of the error between the MBR and the integrated PDV for all 8 consecutive time slices shown in figure 6. The source of the error is the additional 20 km dispersion between each consecutive time slice. (b) shows the result of the data after the dispersion correction is applied to the data.

From the results in figure 8(a), a correction to the displacement can be made. The shift in the displacement data, x, is velocity dependent and can be expressed as $x_{corr}=(x-cvn)$ where x_{corr} is the chromatic dispersion shifted correction, v is the instantaneous velocity, n is the integer multiple of 20 km, and c is a calibration constant. For the Dicon-built ROADDMs, and the results of our flyer plate tests, c was found to be 500 ns for every time slice. After applying this correction, the results in figure 8(a) all shift to zero error as seen in figure 8(b).

Finally, with the Gen4 MPDV system, high power light was able to be launched for the experiments listed in this document. Previous flyer plate tests conducted with the Gen3 MPDV system were limited to 10 mW launch power while the Gen4 MPDV system is capable of launch power up to 200 mW. This represents up to a 20 times increase in the SNR. It should be noted that the noise itself does not increase even with an increase in the laser launch power. For the results shown in figures 6 and 8 above, 100 mW was launched which represents a 10 times

improvement from the previous Gen3 MPDV experiments. Figure 9 shows a comparison between the Gen3 and Gen4 MPDV systems for a nearly identical flyer plate experiment.

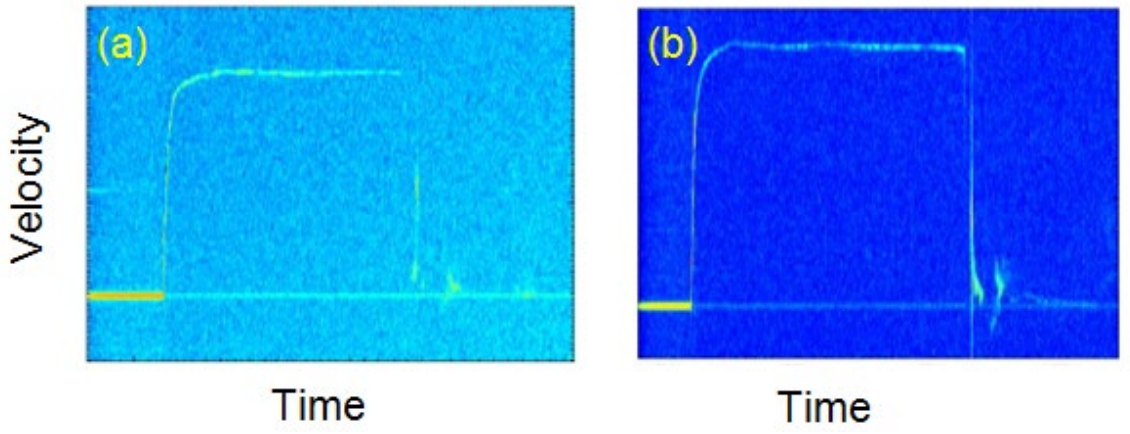

Figure 9 (a) The results of a flyer plate test of identical design as described in this paper with the Gen3 MPDV system. (b) The results of another flyer plate as recorded on the same channel as the results in (a) but with the Gen4 MPDV system.

The results shown in 9(a) represent a 9 dB SNR for the Gen3 MPDV system, while the results in (b) represent a 19 dB SNR for the Gen4 MPDV system. This is close to the theoretical maximum improvement we would expect to see by launching 10 times the laser power. Overall this represents a significant improvement from the previous Gen3 MPDV system.

CONCLUSIONS

In conclusion, a 128 point Gen4 MPDV, capable of launching up to 200 mW power has been installed at DARHT. All 128 points have been fully tested. In addition to the high power MPDV, 128 points of MBR have also been installed. The points have been fully calibrated for all known phase errors including the photodetector phase shifts and the chromatic dispersion inherent in the new ROADDMs. A dispersion constant of 500 ns that is applied to each 20 km length has been calculated. This is also a more uniform result as compared with the results from the Gen3 MPDV system which varied as much as 9% from one time slice to the next.

The photodetector phase corrections for all of the photodetectors have been saved as part of the standard data package for all future MBR tests.

REFERENCE

1. K. Rainey, S. Gilbertson, D. Kalb, and T. Beery, “Modulation based ranging for direct displacement measurements of a dynamic surface”. *Opt. Exp*. **29**, 21174 (2021).